

Flow Characteristics at Asymmetric Sudden Contraction

Abdel-Azim M. Negm

Associate Professor, Dept. of Water & Water Structures Eng.,
Faculty of Engineering, Zagazig University, Zagazig, Egypt
Tel/Fax: +2055 353747; E-mail: abdel_azimn@hotmail.com

Abstract

In this paper, the flow characteristics due to asymmetric sudden contraction is discussed based on experimental investigation when the flow through the contracted section passed from subcritical to critical flow. The experiments are conducted on a 30 cm wide, 45 cm deep and 10.5 m long laboratory flume. Different contraction ratios are considered. Different lengths of the contracted section are tested. Each particular model is tested under the same flow conditions to make the comparisons clear, consistent and logical. Flow characteristics such as discharge coefficient, heading up and energy loss are dealt in. The effects of the flow and contraction parameters on the flow characteristics are presented and discussed. Smaller contraction ratios produce smaller discharge coefficient and causes larger energy loss when compared to bigger contraction ratios.

Keywords: Hydraulics, Transition, Open Channel, Hydraulic Structures, Energy loss, Hump, Box Type Wing walls.

INTRODUCTION

In the design of hydraulic structures, designers do their best to avoid sudden transition of the flow by sudden contractions to ensure smooth flow with minimum energy loss and reduced turbulence patterns. In some cases, sudden contraction is desired (if the location is technically feasible) to reduce the construction cost of the structure since smooth transition needs long structure. An example is the box type wing walls of the bridges. Asymmetric contraction exists in case of flow diversion when the construction is needed in a part of the channel and the flow is running in the other part. The flow through the contracted section may be critical, subcritical or supercritical with subcritical flow upstream.

The change in the cross section disturbs the flow in the contracted reach and near to it from both upstream and downstream. The change in the channel cross section, slope, and/or alignment over a specified reach is termed local transition. Such channel transition are used mainly to avoid or minimize the excessive energy loss, to eliminate the cross waves, the resulting turbulence and to ensure safety of both the structure and the downstream channel reach, Engelund and Petersen (1953). Studies on channel transitions and design of flume inlets include those of Hinds (1928), Ippen (1955), Smith (1967) and Vittal and Chiranjeevi (1983).

The review of literature showed that many studies concerning channel contraction or constriction were published [1-20]. Kindsvater, Carter and Lacy (1953) and Kindsvater and Carter (1955) carried out an experimental investigation to address the effects of different types of contractions on discharge characteristics. Formica (1955) tested experimentally the various design for channel transition (contraction and expansion). The main results of Formica work are reported in Chow (1959). Vallentine

(1958) investigated the effect of then plate contraction placed normal to channel axis. His observations covered data that include different regimes of flow. Laursen (1970) studied the contraction coefficient at sudden expansion at bridge locations. Four distinct flow zones (accretion, contraction, expansion and abstraction) were identified and discussed. It was found that the contraction coefficient varies between 0.7 for about 30% contraction ratio and 1.0 for no contraction. The use of different constrictions for peak discharge measurement by indirect methods was discussed by Matthi (1976) and was outlined in French (1986). Hager and Dupraz (1985) derived a theoretical equation for obtaining the coefficient of contraction in terms of the contraction ratio, the inlet angle of the contraction and the length ratio of the contracted reach. The flow conditions were those of transitional flow from subcritical to supercritical passing through critical at the minimum depth point through the contraction length. They verified their expression experimentally. Alsamman (1989) investigated the effects of the inlet angle of transition, contraction ratio and transition length ratio on the coefficient of contraction based on experimental data when the contraction is asymmetric and the flow upstream is subcritical and passes by critical flow through the transition length. It was concluded that the coefficient of contraction decreases by decreasing the contraction ratio and by increasing the transition inlet angle from 30° to 90° . The transition outlet angle shows insignificant effect on the coefficient of contraction. The transition length ratio, L/b , shows no remarkable effect on the contraction coefficient. Comparing the experimental results of Alsamman (1989) with the equation developed by Hager and Dupraz (1985), it was observed that their equation slightly overestimate the coefficient of contraction by about 2% to 5%, Alsamman (1989).

Recently, Attia (2000) investigated experimentally the effect of variable tailwater conditions at the same discharge on the energy loss through sudden lateral transition. Also, his study indicated that the inlet angle has a pronounced effect on the energy loss upto an angle of about 30° with a slight effect in the range from 30° to 45° and minor effect of greater angles assuming the incoming flow is constant but varying upstream Froude number due to the change in the tailwater depth. Also, Attia and Ibrahim (2000) used the Laser Doppler Velocimetry (LDV) to study the effect of channel contraction on turbulence characteristics. They concluded that the turbulence intensities just upstream of the contraction are higher for smaller contraction ratios (b/B) than for bigger ones. Within the transition, the turbulence intensities increase with decreasing contraction ratio and they are larger in the downstream expansion for smaller contractions.

In the present investigation, the effects of horizontal asymmetric channel contraction on the flow characteristics are presented and discussed based on experimental observations. This works extends what have been started by Hager and Dupraz (1985) and Alsamman (1989) for asymmetric sudden contraction when the flow changes from subcritical to supercritical through the contracted leach of the channel. Their work was concentrated on the coefficient of contraction while our study aims at investigating the energy loss and discharge coefficient characteristics due to the change of both channel contraction and contraction length.

THEORETICAL STUDY

Energy Loss Considerations

Figure 1 shows a definition sketch of flow through local sudden asymmetric side contraction in horizontal channel. The variable affecting the flow through the transition are shown on the figure and explained at the notation section. The functional relationship of the energy loss through transition could be written as follows:

$$f_1(g, V_u, h_u, h_c, b, B, X, L_c, \Delta E) = 0 \quad (1)$$

Using the dimensional analysis, the following nondimensional relationship is obtained:

$$\frac{\Delta E}{h_u} = f_2\left(F_u, \frac{h_c}{h_u}, \frac{b}{h_u}, \frac{B}{h_u}, \frac{X}{h_u}, \frac{L_c}{h_u}\right) \quad (2)$$

Keeping in mind the properties on the non-dimensional quantities, the following expression could be obtained from Eq.(2)

$$\frac{\Delta E}{h_u} = f_3\left(F_u, \frac{h_u}{h_c}, \frac{b}{B}, \frac{X}{L_c}\right) \quad (3)$$

It may be appear better to analyze the energy loss through the transition as a ratio related to the upstream energy, E_u or the critical energy if it occur somewhere in the contracted reach. Therefore, the E_c is used instead of h_u and E_d in the left hand side of equation (3) which becomes:

$$\frac{\Delta E}{E_c} = f_4\left(F_u, \frac{h_u}{h_c}, \frac{b}{B}, \frac{X}{L_c}\right) \quad (4)$$

The energy loss is computed using the following expression:

$$\Delta E = h_u + \frac{V_u^2}{2g} - 1.5h_c \quad (5)$$

where V is the velocity at the point where the depth of flow is h with u for just upstream the contraction and c denotes for the critical conditions.

Similar to Eq.(4), the following equation can be written:

$$\frac{\Delta h}{h_c} = f_5\left(F_u, \frac{h_u}{h_c}, \frac{b}{B}, \frac{X}{L_c}\right) \quad (6)$$

With $\Delta h = h_u - h_c$

Discharge Characteristics Considerations

Apply the energy equation between two sections, one upstream from the contraction and the second at a point through the contracted length. The energy equation takes the form:

$$h_u + \frac{V_u^2}{2g} = h_{cs} + \frac{V_{cs}^2}{2g} + h_L \quad (7)$$

Solving for V_{cs} , keeping in mind that $h_u V_u = y_{cs} V_{cs}$, one obtains:

$$V_{cs} = \sqrt{2g(h_u - h_{cs}) + h_a + h_L} \quad (8)$$

where h_a is the head of approach, $h_a = V_u^2 / 2g$, with V_a being the velocity of approach, $V_u = Q/Bh_u$

Multiplying both sides by the cross sectional area at the critical depth location, neglecting the head loss and use a coefficient of discharge to account for the neglected head loss, the following expression for discharge is obtained:

$$Q = C_d b h_{cs} \sqrt{2g(h_u - h_{cs}) + h_a} \quad (9)$$

where the suffix cs stands for a contracted section or a point through the contracted reach where the depth of water is h_{cs} and the velocity is V_{cs} . If $h_{cs} = h_c$, the discharge could be obtained directly from the relationship between the unit discharge and the critical depth in rectangular channel. However, in this study, h_{cs} is assumed to be equal to h_c and the discharge coefficients are calculated using Eq.(9) to investigate the variations of C_d evaluated based on the critical depth.

EXPERIMENTAL PROGRAM

The experimental work were conducted in a tilting glass sided flume 30 cm wide, 45 cm deep and 10.5 m long. The discharge was measured using a pre-electronic flowmeter. Depth measurements were taken using a needle point gauge with a reading accuracy of ± 0.1 mm. The downstream adjustable tailgate was kept fully open during the experimental program of this study.

The experiments were carried out using three different lateral contraction ratios, b/B , of 0.33, 0.50 and 0.667. For each contraction ratio, the model length is varied three times such that for $b/B=0.33$, $L/b=1, 3$ and 5 , for $b/B=0.50$, $L/b=0.33, 1, 3$ and for $b/B=0.667$, $L/b=0.5, 1$ and 2 . Added to the above, another model having $L/b=0$ at $b/B=0.667$ is test. Actually L here is very small as a thin plat is used to create the contraction from one side, therefore, L/b tends to zero.

For each combination of asymmetric contraction ratio and relative length of contracted length, L/b , flow rates ranging from 300 lit/min to 1500 lit/min were used. The upstream Froude number ranges from about 0.13 to about 0.36. The flow through the transition passes through critical state, thus a critical depth is observed through the transition and the flow changes to supercritical flow and continues supercritical downstream from the sudden expansion section to some distance and a hydraulic jump be formed.

For each combination of contraction ratio and relative length of contraction, the flow rate and the water depth upstream the contraction were measured. It observed that for higher discharge and smaller relative length of contraction, the critical depth may be created downstream from the expansion section for few sets of observations. For this reason, the water surface profiles along the contraction length were measured for few representative runs.

ANALYSIS OF RESULTS AND DISCUSSIONS

Energy Loss Characteristics

The energy loss ratio defined by $(E_u - E_c)/E_u$ is plotted versus the upstream Froude number, F_u , for different contraction ratios, b/B , and for different relative length of contraction, L/b , for each contraction ratio, b/B in Fig.2. The trend of variation of the energy loss ratio with F_u is linear with decreasing trend and separate line for each contraction ratio. At constant b/B , the variations of the energy loss ratio decreases with the increase of F_u and the rate of decrease is higher for lower relative length of contraction, i.e. more energy loss is associated with $L/b=5$ than for $L/b=1$ at fixed b/B . Also, the figure indicates that the higher the contraction ratio, the lower is the energy loss, i.e. $b/B=0.33$ produces more energy loss than $b/B=0.67$ which is true due to the fact that the turbulence intensities increases at the lower contractions, Attia and Ibrahim (2000). It may be interestingly to study the variations of the energy loss with the relative backed up depth $(h_u - h_c)/h_c$ as shown in Fig. 3. An increasing linear trend is observed with separate line for each b/B . At constant backed up depth ratio, the ratio of energy loss increases by increasing the contraction ratio with more increase in the energy dissipation as L/b increases. At constant b/B , the energy loss increases with the increase of the backed up depth ratio.

The variations of the energy loss ratio $(E_o - E_c)/E_c$ with L/b for different contraction ratios are shown in Fig. 4. Similar trend of energy loss variation for both L/b and L/B as both b and B are kept constant for the same b/B and the difference is only in the plotted range of the relative length of contraction. Clearly, the energy loss ratio increases slightly nonlinearly with the increase of L/b or L/B and the variation tends to be negligible at $L/b > 4.0$ and $L/B > 1.50$. Fig. 5(a) indicates the relationship between the percent energy loss and L/b at $Q=300$ liter/min while Fig. 5(b) shows the relationship percent energy loss with L/B at $Q=1500$ liter/min. In Fig. 5, b/B varies between 0.33 and 0.67. Also, the fact that the lower the contraction ratio, the higher is the energy loss at constant L/b is very clear from both figures and from Fig. 6, where $L/b=1.0$. It should be mentioned that at constant b/B , the vertical scatter in the data is due to the variation of the upstream Froude number or the incoming flow capacity.

The Discharge Characteristics

The asymmetric contraction can be used to estimate the discharge passing through the channel by using equation (9) once the discharge coefficient of the contraction is known. The variation of C_d with F_u for different b/B and different L/b for each b/B is shown in Fig. 7. It is noticed that at constant b/B , C_d increases linearly with the increase of F_u and the rate of increase is steep and is high for smaller L/b . The smaller the contraction ratio, the smaller is the discharge coefficient and vice versa. The smaller contraction ratio produces more backed up depth upstream of the contraction. Therefore, the higher the upstream depth ratio, the lower is the discharge coefficient as shown from Fig. 8.

Similar to the case of the percent energy loss, the variations of C_d with L/b (and similarly with L/B) are shown in Figs. 9. The discharge coefficient decreases nonlinearly with the increase of L/b (or L/B) and the rate of increase is high for smaller L/b (or smaller L/B) with insignificant increase in C_d at $L/b > 4$ (or at $L/B > 1.5$).

The vertical scatter at constant b/B and fixed L/b (or L/B) is mainly due to the variations of Froude number of incoming flow capacity as in the case of the energy loss. The relationships between C_d and L/b at constant $Q=300$ liter/min and between C_d and L/B at constant $Q=1500$ liter/min are shown in Figs. 10(a) and 10(b) respectively. Also, in Figure (10), b/B varies between 0.33 and 0.67. Figure 11 presents the relationship between C_d and b/B at $L/b=1.0$ which indicates that C_d is higher for larger contraction ratios. This is due to the lesser rate of energy loss as discussed above.

Backed Up Depth

Furthermore, Fig. 12 presents the variations of the backed up depth ratio with the upstream Froude number, F_u . The lower the contraction ratio, the higher the backed up depth ratio with decreasing trend as F_u increases and the smallest values of C_d for the lowest values of L/b at constant b/B . Also, higher contraction ratio (wider waterway passage) and smaller relative contraction length, produces the smallest backed up depth ratio as in the case of $b/B=0.67$ and $L/b=0.0$.

Water surface Profile

The water surface profiles along the contracted length are measured for $L/b=5.0$ at $b/B=0.33$, for $L/b=3.0$ at $b/B=0.5$ and for $L/b=2$ at $b/B=0.67$. The dimensionless water surface profiles as h/h_u versus X/L are shown in Figs. 13(a,b,c) for the three above mentioned cases respectively. The dimensionless profiles follow a polynomial of second order in the form:

$$\frac{h}{h_u} = a_o + a_1 \left(\frac{X}{L_c} \right) + a_2 \left(\frac{X}{L_c} \right)^2 \quad (10)$$

where a_o , a_1 and a_2 are the regression coefficients and are presented in Table 1 as a function of b/B , L/b and F_u . Alsamman (1989) a similar equation but in dimensional form which makes it of little usefulness.

CONCLUSIONS

An experimental investigation is conducted on the effect of horizontal asymmetric contraction parameters on energy loss and discharge coefficient through the contracted reach in horizontal open channels. The following conclusions may be stated:

- 1- Lower contraction ratios produce more backed up depth ratio with higher values corresponding to bigger values of the relative contraction length at constant contraction ratio.
- 2- Smaller contraction ratios produce more loss of energy at constant relative length of contraction. Higher loss of energy at constant contraction ratios are due to longer contraction length and vice versa.

- 3- Higher contraction ratios produce larger values of C_d at constant relative length of contraction. At constant contraction ratio, lower values of C_d are associated with longer contracted reaches.
- 4- The nondimensional water surface profiles follows a second order polynomial according to Eq.(10) and the drop of water depth through the contraction depends on the contraction ratio, b/B , the relative contraction length, L/b , the upstream Froude number and the relative distance along the contraction, X/L_c .

REFERENCES

- 1- Alsamman, O.M. (1989), Flow characteristics in channel with local contractions, M.Sc. thesis, submitted to Faculty of Engineering, King Saud University, Riyadh, Saudi Arabia.
- 2- Attia, M.I. (2000), Effect of contraction ratio and transition angle on the energy loss in horizontal open channel transitions, Proc. of 5th IWTC 2000, March 25-26, 2000, Alexandria, Egypt.
- 3- Attia, M.I. and Ibrahim, A.A. (2000), A study of the effect of channel contraction on turbulence characteristics using Laser Doppler Velocimetry, Scientific Bulletin, Faculty of Engineering, Ain Shams University, Cairo, Egypt, Vol. 35, No. 2.
- 4- Chow, V.T. (1959), "Open-Channel Hydraulics", McGraw-Hill Book Co., New York, pp. 461-468.
- 5- Engelund, F.A. and Petersen, J.M. (1953), Steady flow in contracted and expanded rectangular channels, La Houille Blanche, Vol. 8, No. 4, p. 464.
- 6- French, R.H. (1986), "Open-Channel Hydraulics", McGraw Hill Book Co., New York, pp.394-421.
- 7- Formica, G., (1955), Preliminary tests on head losses in channels due to cross sectional changes, L'Energia Elettrica, Milano, Vol. 32, No. 7, pp. 554-568, July (in French).
- 8- Hager, W.H. and Dupraz, P.A. (1985), Discharge characteristics of local discontinuous contractions: I, JHR, Vol. 23, No. 5, pp. 421-433.
- 9- Hager, W.H. (1987), Discharge characteristics of local discontinuous contractions: II, JHR, Vol. 25, No. 2, pp. 197-214.
- 10- Hinds, J. (1928), The hydraulic design of flume and syphon transitions, Trans. ASCE, Vol. 92, pp. 1423-1459.
- 11- Ippen, A.T. (1950), Channel transitions and control, in Engineering Hydraulics by H. Rouse, editor, John Wiley and Sons, Inc., New York, Ch.8.
- 12- Kindsvater, C.E., Carter, R.W., and Lacy, H.J. (1953), Computation of peak discharge at contraction, Geological survey Circular, 284-, Washington, D.C.
- 13- Kindsvater, C.E., and Carter, R.W. (1955), Tranquil flow through open channel constrictions, Trans. ASCE, Vo. 120, p. 955.
- 14- Laursen, E.M. (1970), Bridge backwater in the wide valleys, Proc. ASCE, J. Hyd. Div., Vol. 96, HY4, pp. 1019-1038.
- 15- Mathi, H.F. (1976), Measurements of peak discharge at width contractions by indirect methods, Techniques of Water-Resources Investigations of the United State Geological Survey, U.S. Geological Survey, Washington.

- 16- Nagler, F.A. (1981), Obstruction of bridge piers to flow of water, Trans. ASCE, Vol. 82, p. 334.
- 17- Tracy, H.J. and Carter, R.W. (1955), Backwater effects of open channel constrictions, Trans. ASCE, Vol. 120, p. 993.
- 18- Smith, C.D. (1967), Simplified design for flume inlets, Journal of Hydr. Div., ASCE, Vol. 93, HY6, pp. 25-34, Discussions: Vol. 94, HY3, pp. 813-815, Vol. 94, HY4, pp.1152-1153, Vol.94, HY6, pp.1544-1545, Vol. 95, HY4, pp. 1456-1457.
- 19- Vallentine, H.R. (1958), Flow in rectangular channels with lateral constriction plate, La Houille Blanche, Vol. 13, pp. 75-84
- 20- Vittal, N. and Chiranjeevi, V.V. (1983), Open channel transitions: rational methods of design, Journal of Hyd. Div., ASCE, Vol. 109, No. 1, HY1, pp. 99-115.

NOTATIONS

b	width of flume at contracted reach
B	original width of flume
E	energy = $h + V^2/2g$
E_u	upstream energy where the depth is h_u
E_d	downstream energy where the depth of flow is h_d .
F	Froude number
F_u	upstream Froude number at h_u
h	depth of water
h_c	critical depth
h_{cs}	depth of water at a point through the contracted length.
h_u	upstream water depth just upstream of the contraction
h_d	water depth at the end of contraction.
h_L	energy loss = $E_u - E_d$
L_c	length of contracted reach
Q	discharge
q	unit discharge
S_o	bottom slope
V	velocity of flow where the depth is h
V_{cs}	velocity where the depth is h_{cs}
V_u	velocity where the depth is h_u
X	distance along the channel in direction of flow where the depth of water is h

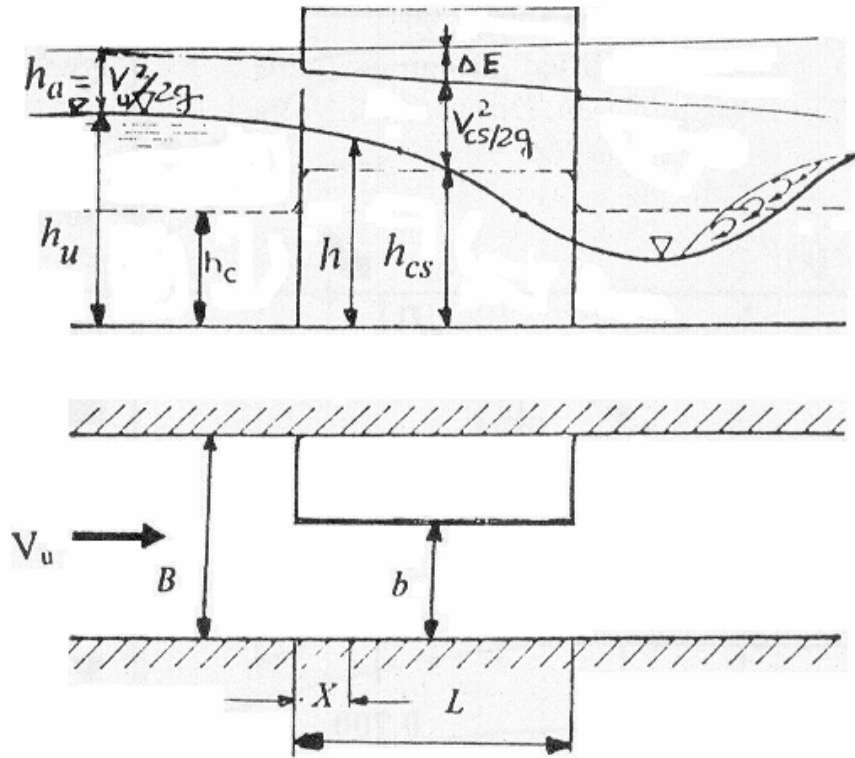


Figure 1. Definition sketch for flow through sudden contraction with subcritical flow in the upstream and supercritical flow in the downstream

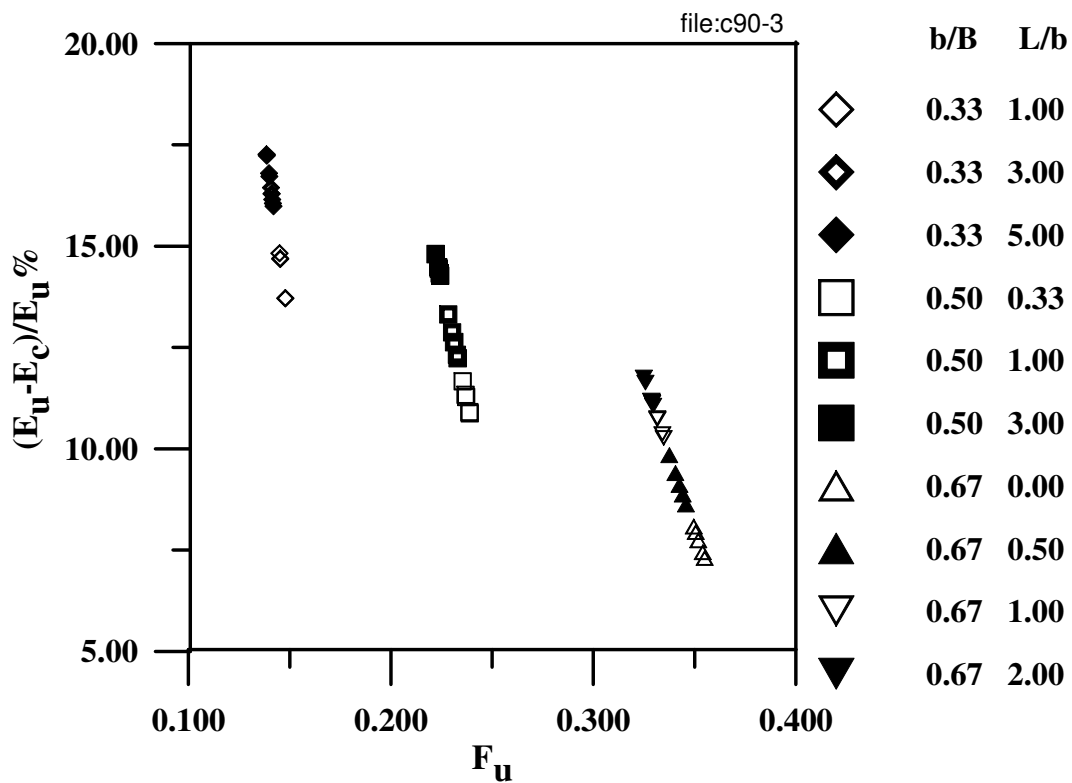


Figure 2. Variation of $(E_u - E_c)/E_u$ with F_u for different b/B and L/b

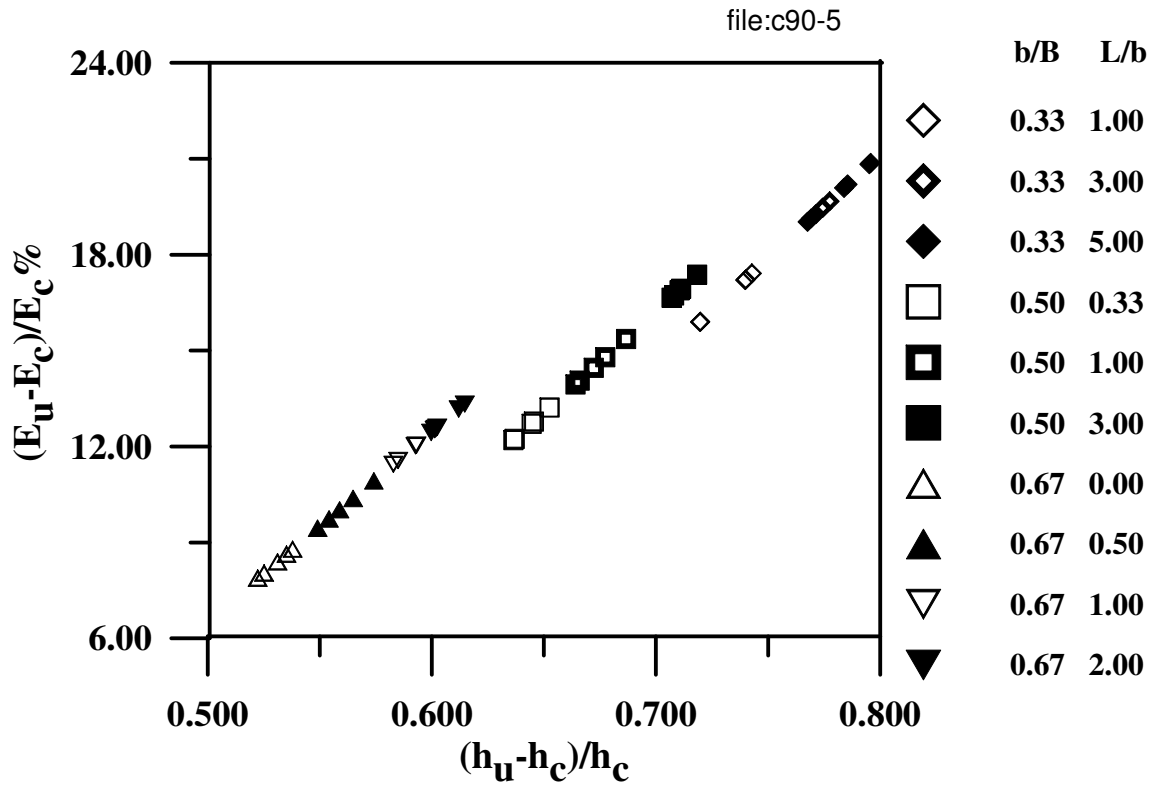


Figure 3. Variation of $(E_u - E_c)/E_c$ with $(h_u - h_c)/h_c$ for different b/B , L/b and variable upstream Froude number, F_u

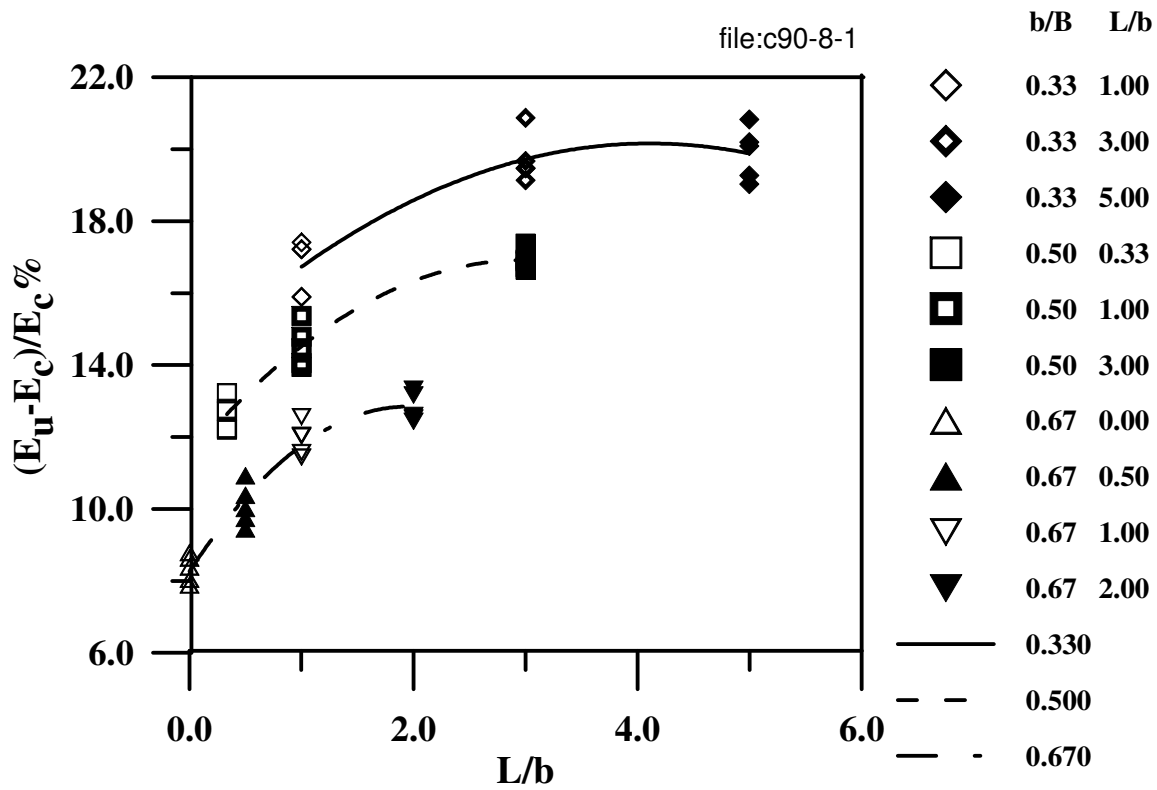


Figure 4. Variation of $(E_u - E_c)/E_c$ with L/b for different b/B and variable F_u

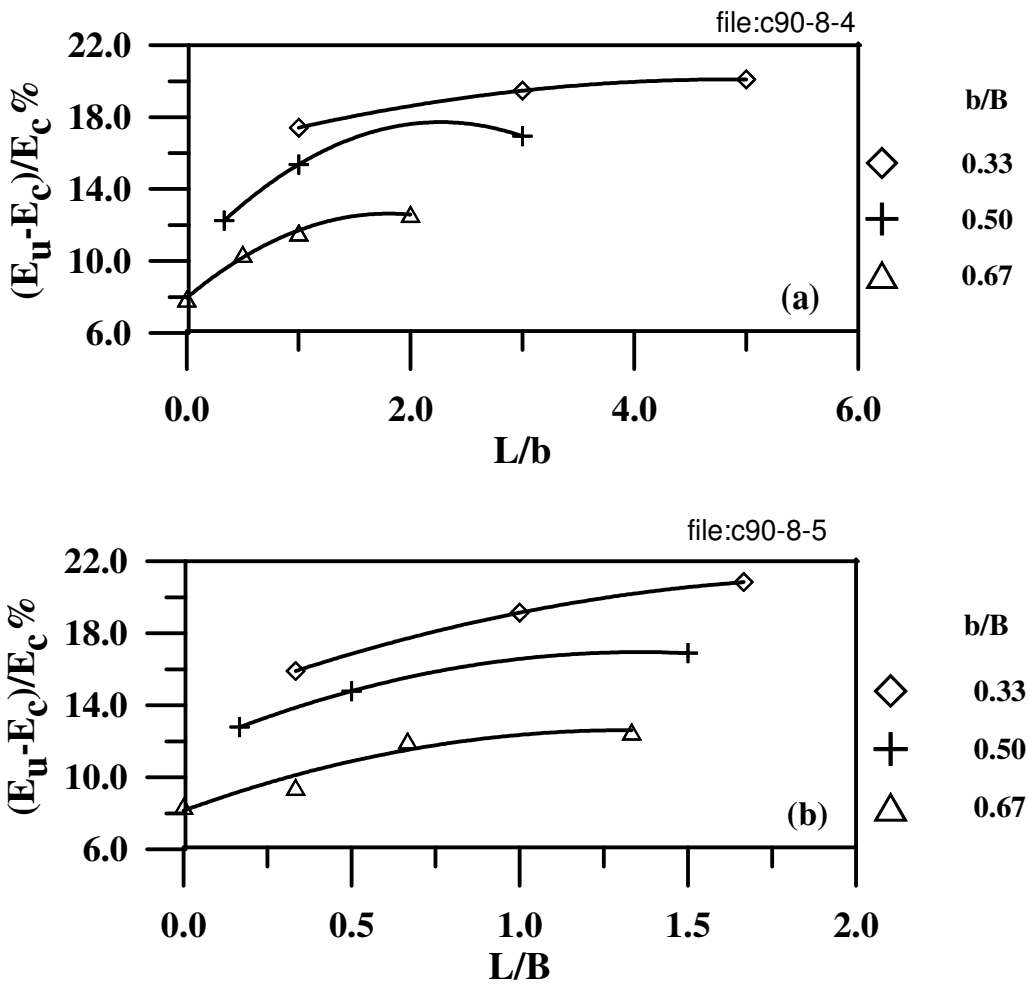


Figure 5. Relationship between $(E_u - E_c)/E_c$ and (a) L/b at $Q=300$ l/m and (b) L/B at $Q=1500$ l/m

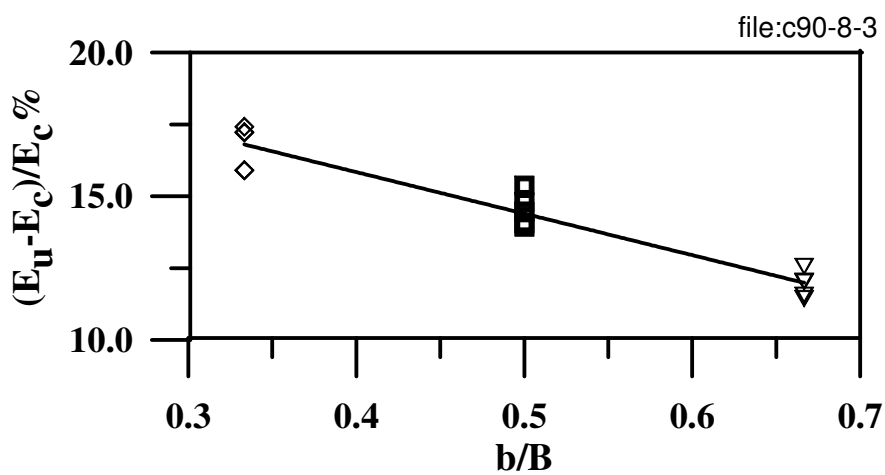


Figure 6. Variation of $(E_u - E_c)/E_c$ with b/B at $L/b=1.0$ and variable F_u

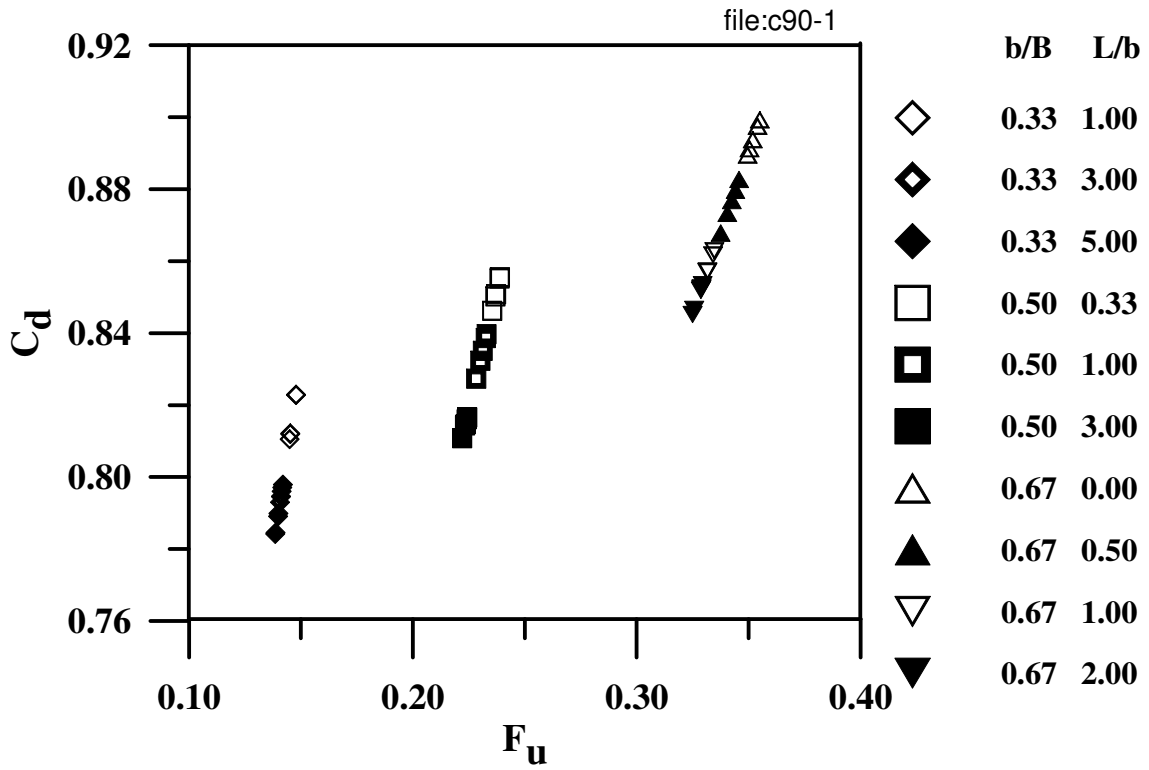


Figure 7. Variation of C_d with F_u for different b/B and L/b

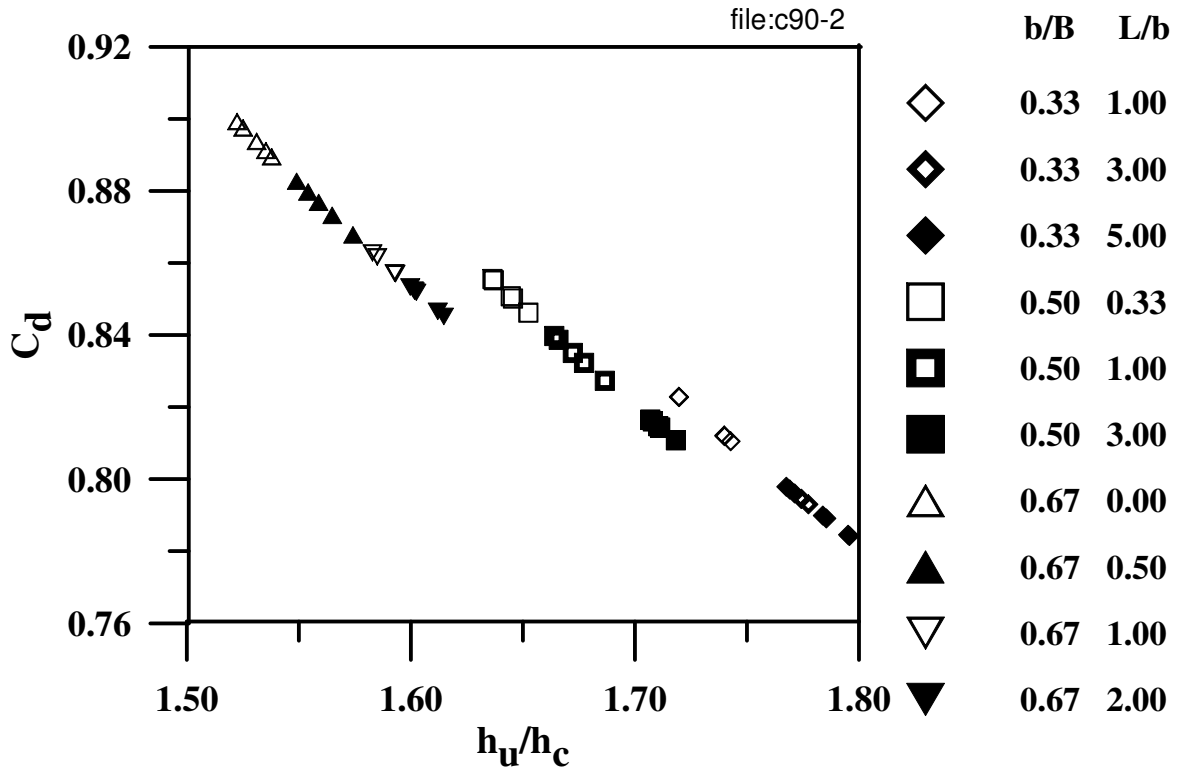


Figure 8. Variation of C_d with h_u/h_c for different b/B , L/b and variable F_u

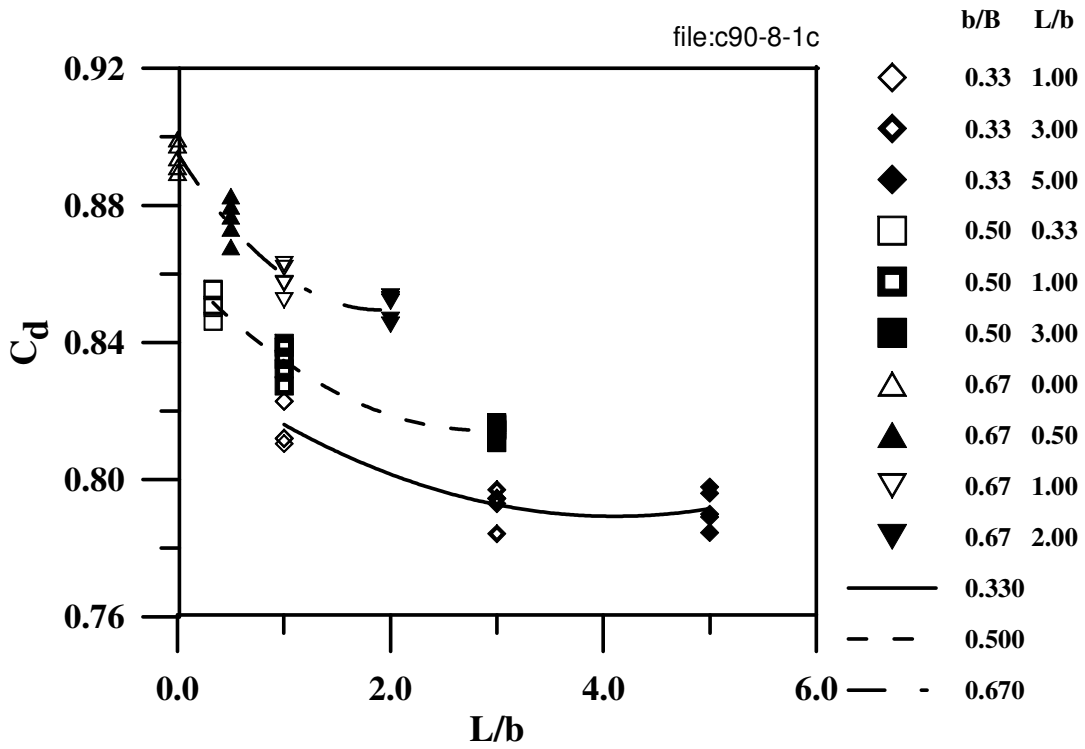


Figure 9. Variation of C_d with L/b for different b/B and variable F_u .

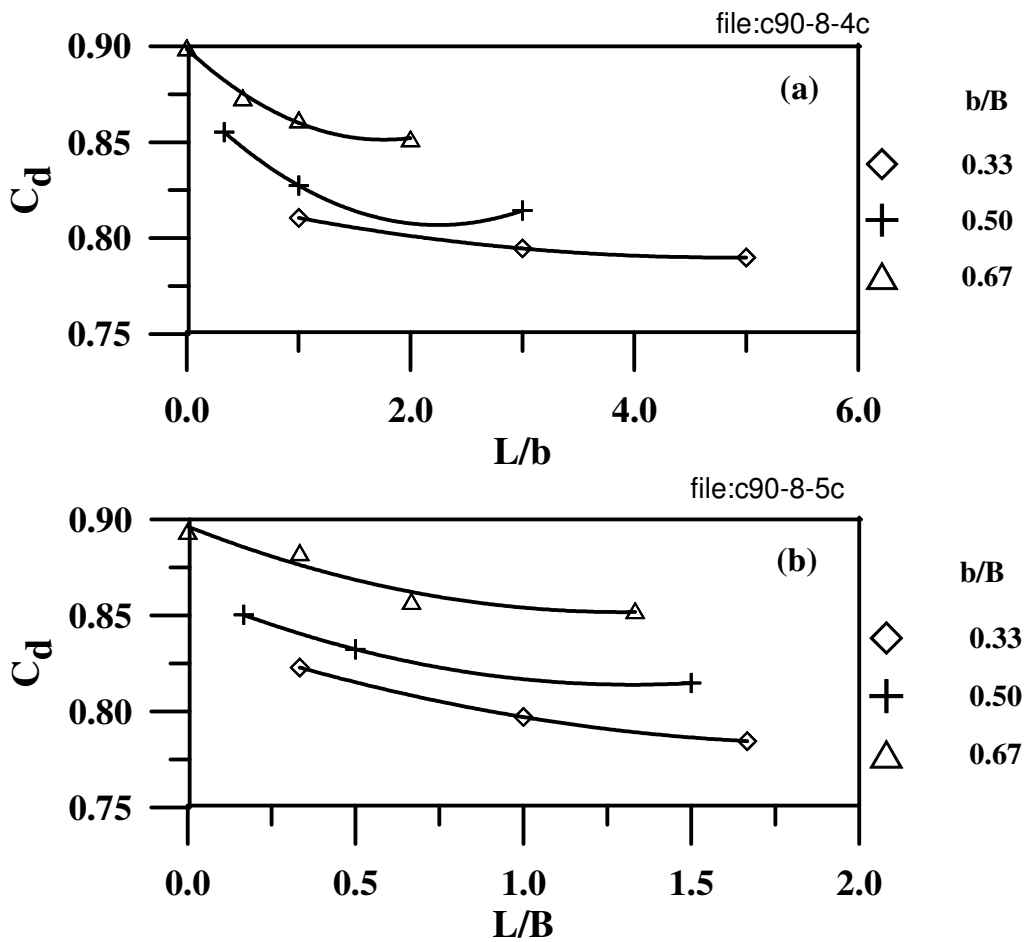


Figure 10. Relationship between C_d and (a) L/b at $Q=300$ l/m (b) L/B at $Q=1500$ l/m

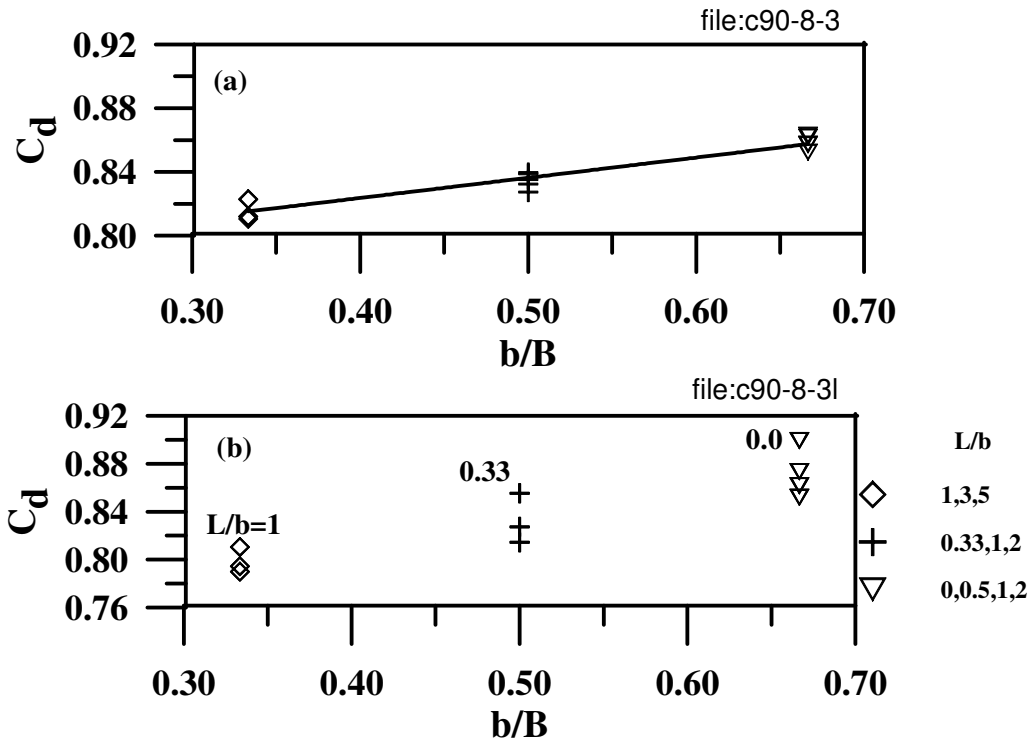


Figure 11. Variations of C_d with b/B for (a) $L/b=1$ and variable Q and (b) Variable L/b and $Q=300$ l/m

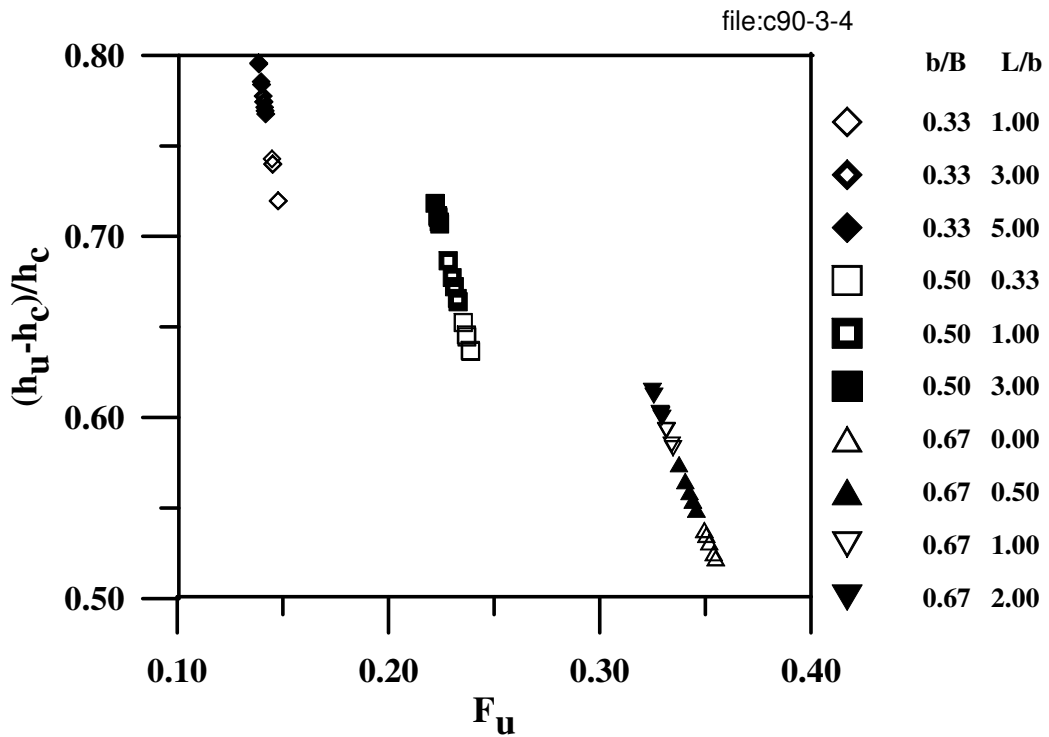


Figure 12. Variations of backed up depth ratio, $(h_u - h_c)/h_c$ with F_u for different b/B and L/b

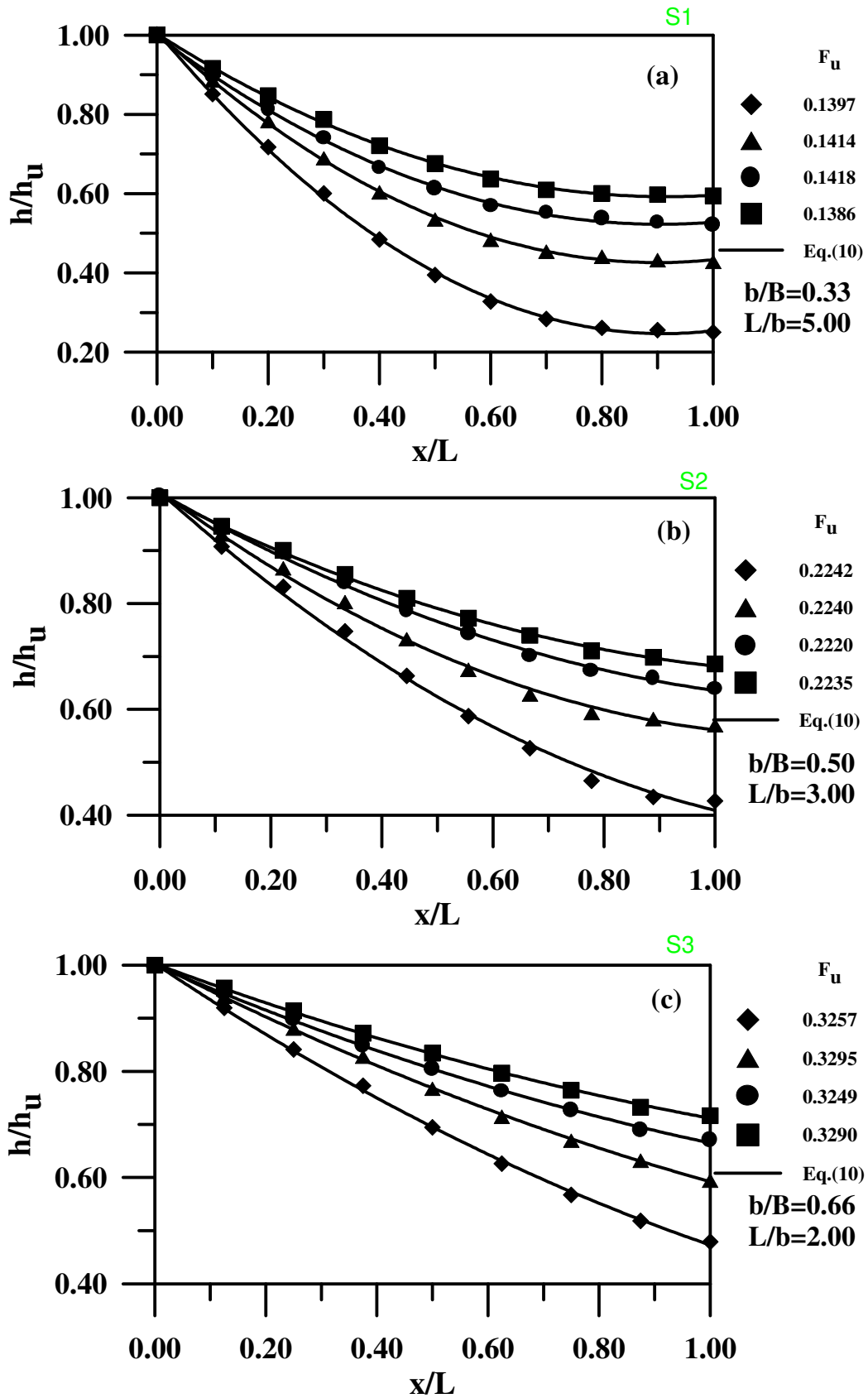


Figure 13. Dimensionless water surface profile along the sudden contraction length